Solar Energy Materials & Solar Cells 104 (2012) 39–44

Contents lists available at SciVerse ScienceDirect

Solar Energy Materials & Solar Cells

journal homepage: www.elsevier.com/locate/solmat

Effect of blend ratio on poly(p-phenylene-ethynylene)-alt-poly (p-phenylene-vinylene) polymer solar cell

Nesrin Tore [a,d], Elif Alturk Parlak [a,*], Ozlem Usluer [b], Daniel A.M. Egbe [c,**], Sait E. San [d], Pelin Aydogan [e]

[a] The Scientific and Technological Research Council of Turkey TUBITAK (National Metrology Institute), Gebze, Kocaeli, Turkey
[b] Department of Chemistry, Mugla University, Kotekli, 48000 Mugla, Turkey
[c] Linz Institute for Organic Solar Cells (LIOS), Physical Chemistry, Johannes Kepler University, Altenbergerstr. 69, A-4040 Linz, Austria
[d] Physics Department, Gebze Institute of Technology, Gebze, Kocaeli, Turkey
[e] Physics Department, Yildiz Technical University, Turkey

ARTICLE INFO

Article history:
Received 22 December 2011
Received in revised form
16 April 2012
Accepted 24 April 2012
Available online 22 May 2012

Keywords:
AnE-PVstat
Polymer solar cell
Blend ratio

ABSTRACT

We investigated the effect of the amount of phenyl C_{61} butyric acid methyl ester (PCBM) on anthracene-containing poly(p-phenylene-ethynylene)-alt-poly(p-phenylene-vinylene) (PPE–PPV) polymer (AnE-PVstat) solar cells. The efficiencies and fill factors of the polymer solar cells improved with increasing PCBM content. The highest efficiency obtained was 2.13% for AnE-PVstat:PCBM solar cells with 75% PCBM content. The increased efficiency for that PCBM content can be attributed to a change in the thin film nanostructure. The normalized efficiency values versus time plot from ISOS-L-1 test indicated that the AnE-PVstat:PCBM solar cell with 1:2 blend ratio showed 100% durability; for 1:3 and 1:4 ratios it showed with approximately 96% durability under standard solar irradiation of 100 mW/cm^2 (AM1.5G) at ambient conditions for 21 h. ISOS-D-3 Damp test indicated that the normalized j_{sc} and normalized efficiency versus time graphs showed similar behaviors; the AnE-PVstat:PCBM solar cell with 1:4 ratio has 99% durability for 40 h in a weathering chamber.

1. Introduction

Poly(p-phenylene-ethynylene)-alt-poly(p-phenylene-vinylene)s (PPE–PPVs) are a new class of conjugated compounds combining the intrinsic properties of both poly(p-phenylene-ethynylene) (PPE) and poly(p-phenylene-vinylene) (PPV) into a single polymeric backbone with additional structure-specific properties.

The PPV backbone involving acetylene units within opened way to new types of conjugated systems denoted as PPE–PPVs, showing outstanding optoelectronic properties [1,2]. This class of compounds has successfully been used either as donor or acceptor components in solar cell devices. Open-circuit voltages, V_{oc}, as high as 950 mV and 1.50 V have been obtained from polymer–PCBM heterojunction cells [3–5] and from polymer–polymer bilayer cells [6,7], respectively. The short circuit currents, I_{sc}, and the filling factors, *FF*, were found to be greatly dependent on the triple bond/double bond ratio as well as the nature and size of the soluble alkoxy side groups [8].

Significant progress in BHJ solar cells has been made by the synthesis of low band gap conjugated polymers and optimization of the device preparation conditions, including the application of adjusting the volume fractions of the components [9–11], thermal annealing treatments [12,13], and solvent annealing [14,15].

The work function of the metal influences the efficiency of organic solar cells, since lowering work function of silver (Ag) using calcium (Ca) metal increases the charge collection at the electrodes [16]. Photovoltaic performances of PPE–PPVs were investigated by Egbe et al. [17] with Aluminum metal electrode (ITO/PEDOT:PSS/active layer/Al). In this letter, we find that 10 nm thick Ca between active layer and Ag increased both open circuit potential (V_{oc}) and fill factor (*FF*), yielding increased power conversion efficiency.

In this study, the blend ratio (AnE-PVstat:PCBM) effect of AnE-PVstat copolymer solar cell on photovoltaic performance was systematically investigated. AnE-PVstat:PCBM solar cells were characterized with UV spectroscopy and atomic force microscopy (AFM). Both dark and under illumination stability tests of AnE-PVstat:PCBM solar cells were also performed.

2. Experimental

2.1. Materials and solutions

The AnE-PVstat polymer (Fig. 1) equally equipped with linear octyl and branched 2-ethylhexyl side-chains at the PPE- and

* Corresponding author. Tel.: +902626795000; fax: +902625001.
** Corresponding author. Tel.: +43 732 2468-8398.
E-mail addresses: elif.parlak@ume.tubitak.gov.tr (E.A. Parlak), daniel_ayuk_mbi.egbe@juk.at (D.A.M. Egbe).

0927-0248/$ - see front matter © 2012 Elsevier B.V. All rights reserved.
http://dx.doi.org/10.1016/j.solmat.2012.04.040

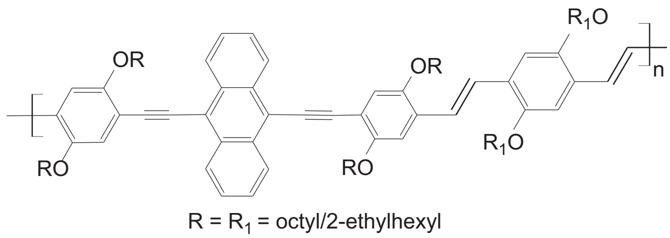

Fig. 1. Chemical structure of AnE-PVstat polymer.

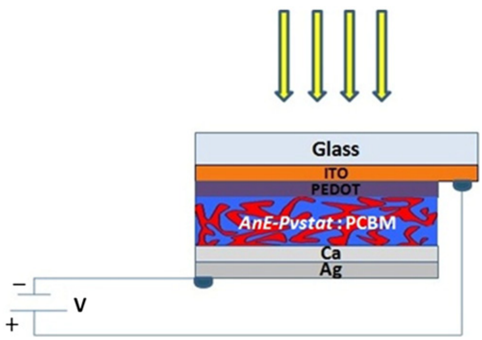

Fig. 2. Device architecture of polymer solar cell.

PPV-parts was synthesized according to procedures described previously [17,18]. The hole transport layer material, poly(3,4-ethylenedioxythiophene) (PEDOT) doped with poly(styrene sulfonic acid) (PSS) (PEDOT:PSS Clevios P500), was purchased from Heraeus and n-type semiconductor phenyl C_{61} butyric acid methyl ester ($PC_{61}BM$) was from Sigma-Aldrich. AnE-PVstat and PCBM solutions with 25 mg/ml concentration were prepared by using 1,2 dichlorobenzene from Alfa Aesar.

2.2. Film and device fabrication

All cells were fabricated on indium tin oxide (ITO) coated glass substrates with a sheet resistance 25Ω/square. The substrates were cleaned in an ultrasonic bath with de-ionized water, acetone, and isopropyl alcohol successively for 5 min and dried by dry nitrogen. After that the hole transport layer PEDOT:PSS was spin coated on the substrates and then annealed at 100 °C on a hotplate for 10 min. The active layer solutions were prepared by mixing the polymer and PCBM in different blend ratios of 1:1, 1:2, 1:3 and 1:4. Then the blends were spin coated on the substrates and annealed at 120 °C for 2 min. The cathode comprising Ca (10 nm) and Ag (100 nm) was deposited through a shadow mask (Fig. 2). Finally, devices were encapsulated with a glass by using Ossila UV-epoxy resin.

2.3. Measurements

The current density–voltage (*j*–*V*) characteristics of devices were taken under light illumination using standard solar irradiation of 100 mW/cm^2 (AM1.5) with Xenon lamp as a light source and a computer-controlled voltage–current Keithley 2600 source meter at 25 °C under an ambient atmosphere. Morphology of the blend films was investigated with atomic force microscopy (Park Systems).

3. Results and discussion

3.1. Photovoltaic performances of AnE-PVstat:PCBM solar cells

The effect of blend ratio on the photovoltaic (PV) parameters of AnE-PVstat:PCBM solar cells is seen in Table 1. It is indicated that

Table 1
Photovoltaic parameters of AnE-PVstat:PCBM solar cells with various blend ratios.

Ratio	V_{OC} (V)	j_{sc} (mA/cm^2)	V_m (*V*)	*Jm* (mA/cm^2)	*FF*	PCE η	R_{sh} (Ωcm^2)	R_s (Ωcm^2)	Thickness (nm)
1:1	0.774	4.78	0.590	3.02	0.48	1.78	534	19.5	292
1:2	0.762	5.19	0.563	3.43	0.49	1.93	539	17.5	245
1:3	0.778	5.04	0.590	3.62	0.54	2.13	644	14.0	170
1:4	0.774	4.33	0.609	3.17	0.57	1.93	637	11.9	135

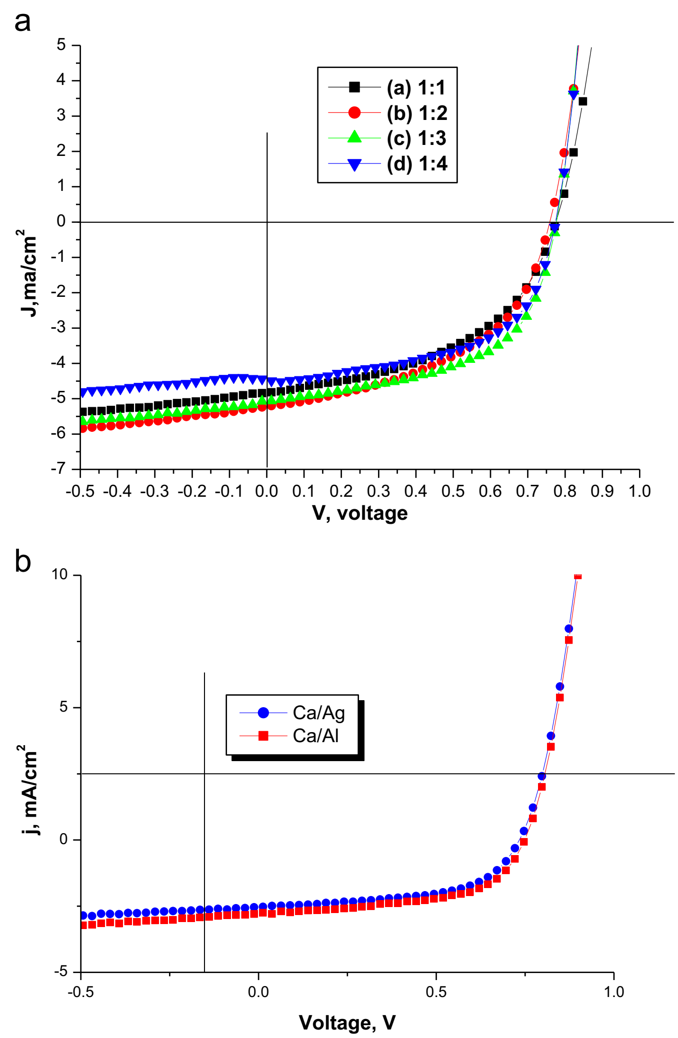

Fig. 3. (a) *j* and *V* characteristics of AnE-PVstat:PCBM solar cells with different composition ratios: (a) AnE-PVstat:PCBM device with 1:1 ratio, (b) AnE-PVstat:PCBM device with 1:2 ratio, (c) AnE-PVstat:PCBM device with 1:3 ratio and (d) AnE-PVstat:PCBM device with 1:4 ratio. (b) *j* and *V* characteristics of AnE-PVstat:PCBM solar cells with Ca/Ag and Ca/Al electrodes.

power conversion efficiency (PCE) of both solar cells increased with increasing fullerene compositions until it reached a maximum with PCBM content up to 75 wt%. After that concentration the efficiency started to decline, because of the poor-film forming properties of PCBM; thus the influence of leakage current is large. The evaluation of fill factor as a function of the PCBM concentration is that the overall rise of *FF* with increasing PCBM content indicates smaller series of resistance (R_s) since *FF* rises with weight percentage of PCBM from 0.48 to 0.57.

Typical *j* and *V* characteristics of AnE-PVstat:PCBM solar cells with different composition ratios are shown in Fig. 3a. The highest short circuit current j_{sc} of AnE-PVstat:PCBM device with 50 wt% can be attributed to higher carrier mobility and improved conducting percolation pathway [19]. The change in power conversion efficiency (PCE) with varying composition is of course a straight forward combination of the changes in j_{sc}, V_{oc} and FF and confirms that the cells reach a maximum performance at 75 wt% PCBM. This value is quite close to that of MDMO–PPV:PCBM solar cell with a maximum performance at 80 wt%PCBM [20]. For comparison cathode material, we fabricated AnE-PVstat:PCBM Ca/Al and Ca/Ag solar cells, as we wondererd whether cathode Ag makes any effect on PCE of the solar cells. The results showed that Ca/Ag did not cause any decrease in PCE of solar cells (Fig. 3b).

3.2. Morphology study of AnE-PVstat:PCBM blends

To obtain a deeper insight in the relation between morphology and performance of polymer/fullerene bulk heterojunction solar cells, devices have been characterized via AFM. The AFM topographic images of AnE-PVstat:PCBM blends with different blend ratios : a, 1:1; b, 1:2; c, 1:3;d, 1:4 are shown in Fig. 4. These composition ratios are equal to the weight ratios, that is compositions are 50, 67, 75, 80 wt% PCBM in AnE-PVstat correspondingly. It is indicated that peak to valley values are 3.79, 5.25, 5.85 and 4.44 nm and also rms roughnesses are 0.88, 1.15, 1.26 and 0.92 nm respectively. The highest peak to valley and roughness values were obtained by AnE-PVstat:PCBM blend with 75 wt% . PCBM content. The obvious relation between the device performance and surface roughness of the film is that the higher roughness gives higher efficiency. One possible reason may be the increased contact area between polymer film and metal cathode for the films with higher roughness. The increased contact area has an effect on the charge collection at the metal and polymer interphase [21]. We also take optical microscope images of the devices; it is seen that the amount of PCBM and sizes of PCBM are the highest for the device 1:3 blend ratio (Fig. 5). The big PCBM aggregation is the reason of the higher porosity. This microscopic view of the morphology is correlated with nanomorphology. Several light-trapping approaches on organic solar cells were explored following the developments of

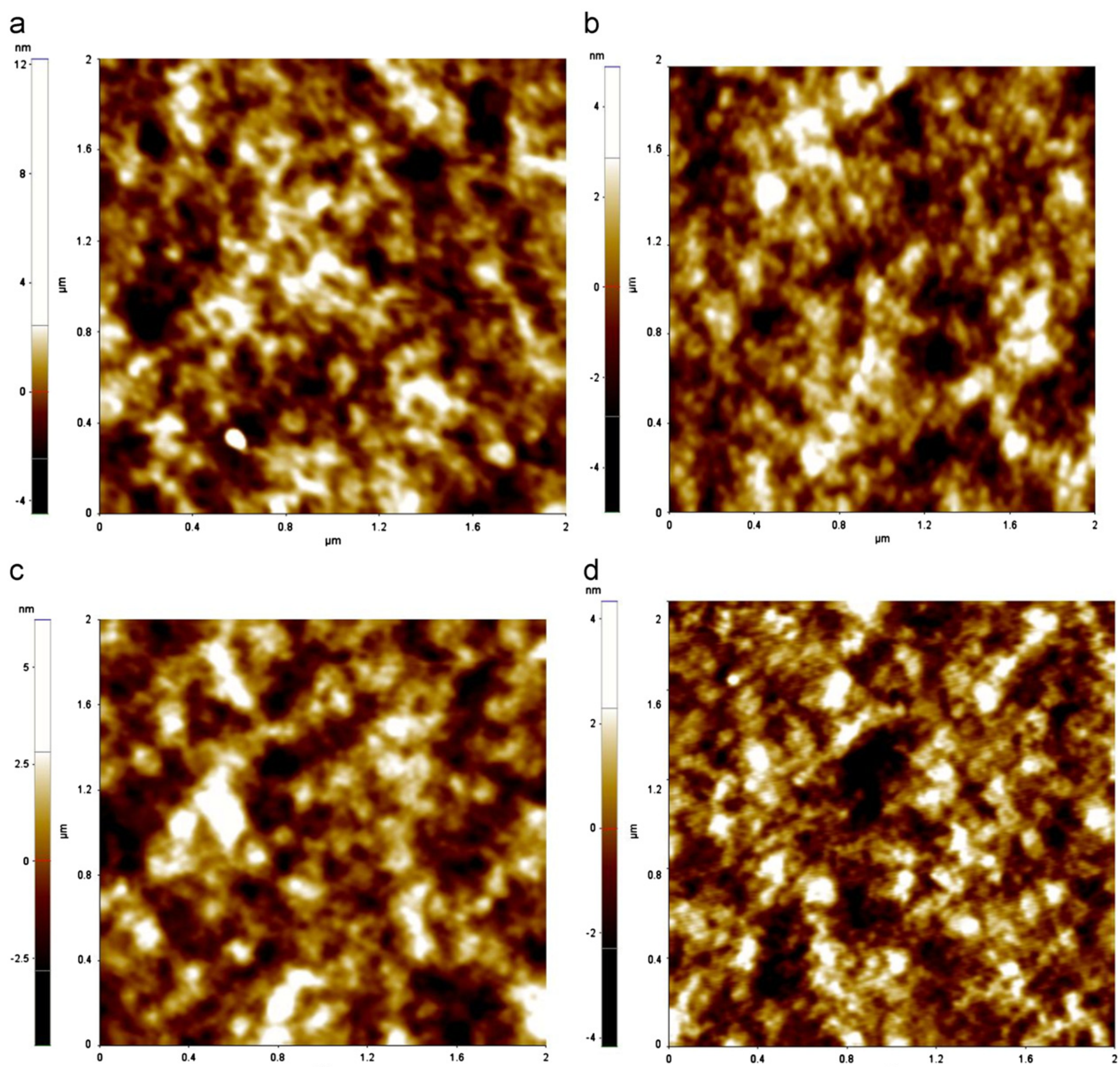

Fig. 4. AFM height images of AnE-PVstat:PCBM solar cells (2 μm–2 μm) with different composition ratios: (a) AnE-PVstat:PCBM device with 1:1 ratio, (b) AnE-PVstat:PCBM device with 1:2 ratio, (c) AnE-PVstat:PCBM device with 1:3 ratio and (d) AnE-PVstat:PCBM device with 1:4 ratio.

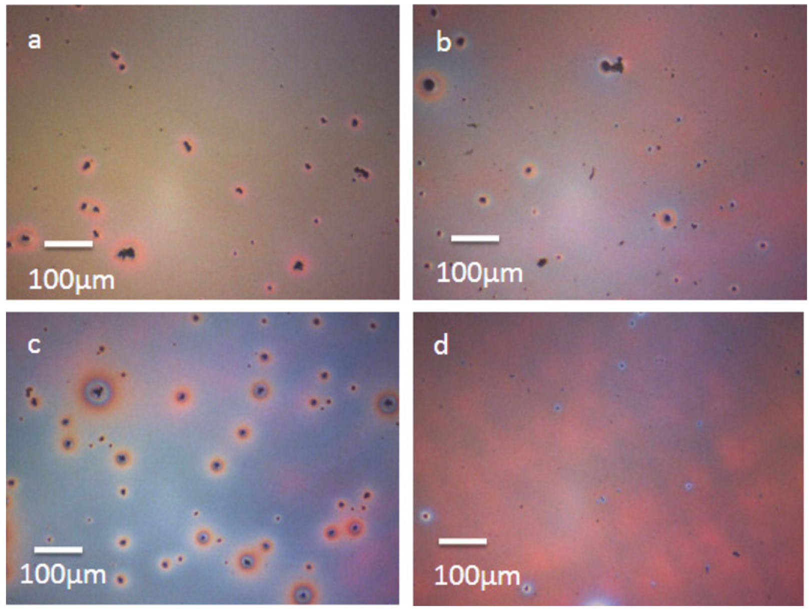

Fig. 5. Optical microscoscopy images of AnE-PVstat:PCBM solar cells with different composition ratios: (a) AnE-PVstat: PCBM device with 1:1 ratio, (b) AnE-PVstat:PCBM device with 1:2 ratio, (c) AnE-PVstat:PCBM device with 1:3 ratio and (d) AnE-PVstat:PCBM device with 1:4 ratio.

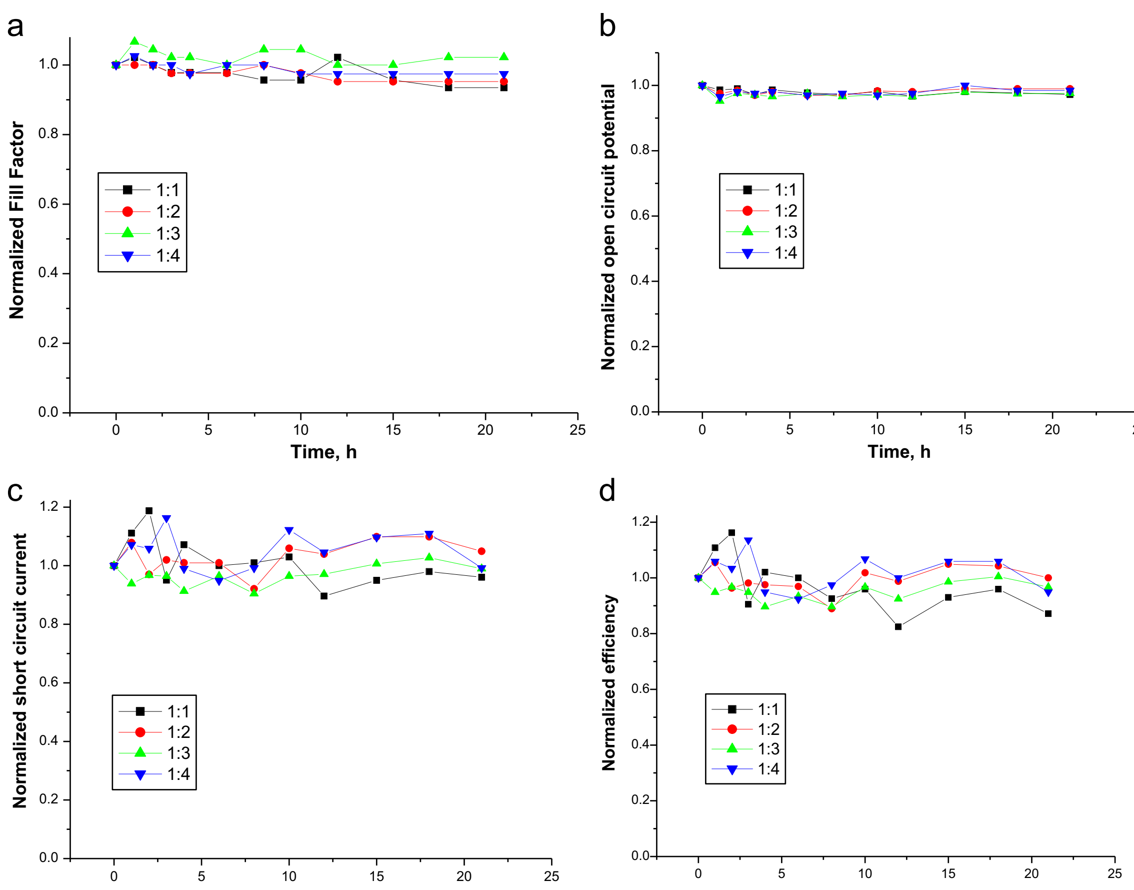

Fig. 6. Stability study of AnE-PVstat:PCBM under standard solar irradiation of 100 mW/cm^2 (AM1.5G) at ambient conditions (a) normalized fill factor versus time graph of AnE-PVstat:PCBM solar cell, (b) normalized open circuit potential versus time graph of AnE-PVstat:PCBM solar cell, (c) normalized short circuit current versus time graph of AnE-PVstat:PCBM solar cell and (d) normalized efficiency versus time graph of AnE-PVstat:PCBM solar cell with different blend ratios.

wave-optics and nanotechnology. By scattering light into active layers with nanoparticles or textured substrates, light absorption has been enhanced generally. In this study, the blend morphology of AnE-PVstat:PCBM with 75 wt% PCBM content is rougher than that at other ratios of solar cells; the rough surface increases light absorption like in the photo-trapping effect.

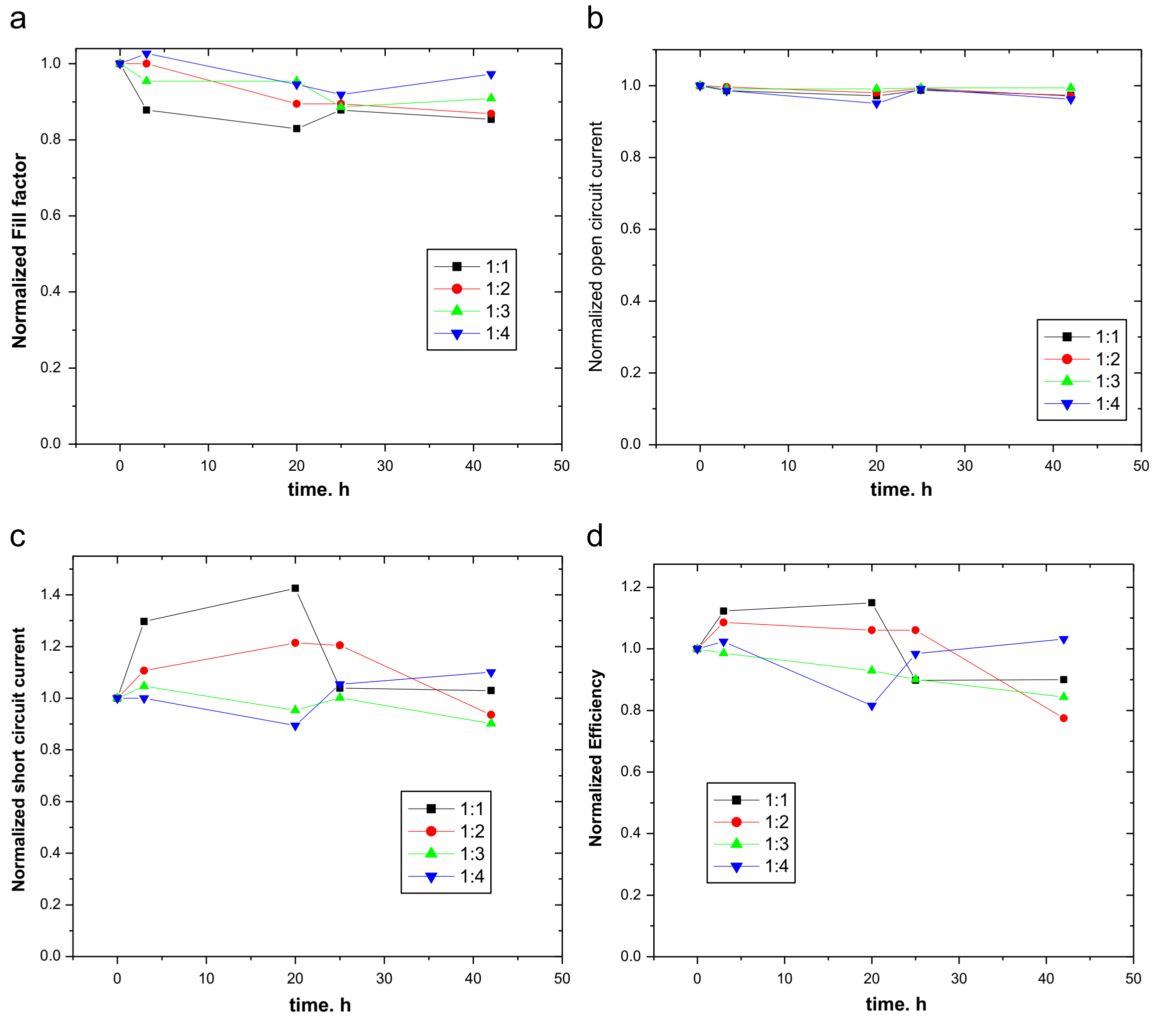

Fig. 7. AnE-PVstat:PCBM solar cell with different composition ratios exposed to 65 °C, 85% moisture in a weathering chamber; (a) normalized fill factor versus time, (b) normalized *Voc* versus time, (c) normalized j_{sc} versus time and (d) normalized efficiency versus time plots with different blend ratios.

3.3. Laboratory weathering testing

For accurate comparison of indoor stability testing in real life, a light source that closely matches spectral distribution of day light has to be chosen. Xenon Arc is very good match to AM 1.5G with correct filter. Since lamp aging tends to affect more in the UV range than in other ranges, monitoring in UV range is critical to maintain proper irradiance level. For indoor testing, ISOS-L-1 [22] was carried out to understand degradation of organic solar cells. ISOS-L-1 testing (Fig. 6) indicated that the short circuit currents of all devices are very stable with durability approximately 95%; it has small variations for all blend ratios. The normalized efficiency values versus time plot indicated that the AnE-PVstat:PCBM solar cell with 1:2 blend ratio showed 100% durability whereas with 1:3 and 1:4 ratios it should approximately 96% durability. The AnE-PVstat:PCBM solar cell with 1:1 blend ratio has durability 85% which was the smallest but it still has good stability (Fig. 6). Normalized open circuit potential does not change with time for the AnE-PVstat:PCBM solar cell with all blend ratios. ISOS-L-1 test revealed that the AnE-PVstat:PCBM solar cell has very good stability under standard solar irradiation of 100 mW/cm^2 (AM1.5G) at ambient conditions for 21 h. In literature, it is known that cathode composition affects the stability of polymer solar cell. Bettignies and Guillerez [22] claimed that the Ca/Ag-based cathode is more stable than Al based cathodes. They also allege that organic solar cells using Ca/Ag as a cathode can reach operational life-times of 2400 h under sun illumination [22]; this also supports our idea that Ca/Ag is more stable than Al based cathodes. We have studied the stability of P3HT solar cells with a Ca/Ag electrode in our previous work [23]. ISOS-L-1 testing of P3HT solar cells indicated that the efficiencies and short circuit currents of all devices have small variations.

3.4. Shelf life study

Shelf life studies are carried out by leaving samples in the dark without illumination. We have carried out ISOS-D-3 Damp test [24] for AnE-PVstat:PCBM solar cell stability test in the dark and in a high stress level at 65 °C and 85% moisture. The results indicated that V_{oc} of AnE-PVstat:PCBM solar cell seems very stable during 40 h in the weathering box which is at 65 °C and 85% humidity (Fig. 7). Fill factors of the cells with different blend ratios indicated that 1:3 and 1:4 ratios have approximately 90% durability. The normalized j_{sc} and normalized efficiency versus time graphs showed similar behaviors; the 1:4 ratio cell has 99% durability for 40 h in a weathering chamber (Fig. 7).

4. Conclusion

Blend ratio of (AnE-PVstat):PCBM prominently affects PV performances of organic solar cell. In this work, it is seen that increasing PCBM loading leads to an increase in efficiency and fill factor. A high open circuit potential of this polymer is also an important advantage for obtaining high efficiency for the organic solar cells. The PCBM loading also influences the morphology of AnE-PVstat:PCBM active layer; the highest peak to valley and roughness values were obtained for the AnE-PVstat:PCBM blend with 75 wt% PCBM content. The higher roughness provided higher efficiency for PPE–PPVs:PCBM solar cells. Both ISOS-L-1 and ISOS-D-3 Damp tests showed that AnE-PVstat:PCBM solar cells have very good stability for a definite time period with greater than 90% durability.

Acknowledgement

D.A.M. Egbe is grateful to the Deutsche Forschungsgemeinschaft (DFG) for financial support in the framework of the priority program SPP1355. Daniel Egbe has been supported by 2221-Visiting Scientist Fellowship Program of TUBITAK.

References

[1] D.A.M. Egbe, C. Ulbricht, T. Orgis, B. Carbonnier, T. Kietzke, M. Peip, M. Metzner, M. Gericke, E. Birckner, T. Pakula, D. Neher, U.-W. Grummt, Odd–even effects and the influence of length and specific positioning of alkoxy side chains on the optical properties of PPE–PPV polymers, Chemistry of Materials 17 (2005) 6022–6032.

[2] E. Tekin, H. Wiljaars, E. Holder, D.A.M. Egbe, U.S. Schubert, Film thickness dependency of the emission colors of PPE–PPVs in inkjet printed libraries, Journal of Materials Chemistry 16 (2006) 4294–4298.

[3] H. Hoppe, D.A.M. Egbe, D. Mühlbacher, N.S. Sariciftci, Photovoltaic action of conjugated polymer/fullerene bulk heterojunction solar cells using novel PPE–PPV copolymers, Journal of Materials Chemistry 14 (2004) 3462–3467.

[4] M. Al-Ibrahim, A. Konkin, H.K. Roth, D.A.M. Egbe, E. Klemm, U. Zhokhavets, G. Gobsch, S. Sensfuss, Phenylene-ethynylene/phenylene-vinylene hybrid polymers: optical and electrochemical characterization, comparison with poly[2-methoxy-5-(3′,7′-dimethyloctyloxy)-1,4-phenylene vinylene] and application in flexible polymer solar cells, Thin Solid Films 474 (2005) 201–210.

[5] D.A.M. Egbe, L.H. Nguyen, B. Carbonnier, D. Mühlbacher, N.S. Sariciftci, Thiophene-containing poly(arylene–ethynylene)-*alt*-poly(arylene–vinylene)s: synthesis, characterisation and optical properties, Polymer 46 (2005) 9585–9595.

[6] D.A.M. Egbe, T. Kietzke, B. Carbonnier, D. Mühlbacher, H.-H. Hörhold, D. Neher, T. Pakula, Synthesis, characterization, and photophysical, electrochemical, electroluminescent, and photovoltaic properties of Yne-Containing CN–PPVs, Macromolecules 37 (2004) 8863–8873.

[7] T. Kietzke, D.A.M. Egbe, H.-H. Hörhold, D. Neher, Comparative study of M3EH–PPV-based bilayer photovoltaic devices, Macromolecules 39 (2006) 4018–4022.

[8] D.A.M. Egbe, L.H. Nguyen, K. Schmidtke, A. Wild, C. Sieber, S. Gunes, N.S. Sariciftci, Combined effects of conjugation pattern and alkoxy side chains on the photovoltaic properties of Thiophene-Containing PPE–PPVs, Journal of Polymer Science Part A: Polymer Chemistry 45 (2007) 1619–1631.

[9] S.H. Park, A. Roy, S. Beaupre, S. Cho, N. Coates, J.S. Moon, D. Moses, M. Leclerc, K. Lee, A.J. Heeger, Bulk heterojunction solar cells with internal quantum efficiency approaching 100%, Nature Photonics 3 (2009) 297–303.

[10] A.C. Mayer, M.F. Toney, S.R. Scully, J. Rivnay, C.J. Brabec, M. Scharber, M. Koppe, M. Heeney, I. McCulloch, M.D. McGehee, Bimolecular crystals of fullerenes in conjugated polymers, Advanced Functional Materials 19 (2009) 1173–1179.

[11] S.S. Van Bavel, M. Barenklau, G. deWith, H. Hoppe, J. Loos, P3HT/PCBM bulk heterojunction solar cells: impact of blend composition and 3D morphology on device performance, Advanced Functional Materials 20 (2010) 1458–1463.

[12] H. Hoppe, N.S. Sariciftci, Morphology of polymer/fullerene bulk heterojunction solar cells, Journal of Materials Chemistry 16 (2006) 45–61.

[13] W.L. Ma, C.Y. Yang, X. Gong, K. Lee, A.J. Heeger, Interdiffusion of PCBM and P3HT reveals miscibility in a photovoltaically active blend, Advanced Functional Materials 15 (2005) 1617–1622.

[14] J. Jo, S.I. Na, S.S. Kim, T.W. Lee, Y. Chung, S.J. Kang, D. Vak, D.Y. Kim, Three-dimensional bulk heterojunction morphology for achieving high internal quantum efficiency in polymer solar cells, Advanced Functional Materials 19 (2009) 2398–2406.

[15] S.S. Van Bavel, E. Sourty, G. de With, J. Loos, Three-dimensional nanoscale organization of bulk heterojunction polymer solar cells, Nano Letters 9 (2009) 507–513.

[16] Y. Jiang, X. WeiSun, D. WeiZhao, A.K.K. Kyaw b, Y.N. Li, Low work function metal modified ITO as cathode for inverted polymer solar cells, Solar Energy Materials and Solar Cells 94 (2010) 1618–1621.

[17] D.A.M. Egbe, S. Turk, S. Rathgeber, F. Kühnlenz, R. Jadhav, A. Wild, E. Birckner, G. Adam, A. Pivrikas, V. Cimrova, G. Knör, N.S. Sarıciftci, H. Hoppe, Antracene based conjugated polymers: correlation between $\pi\rightarrow\pi$-stacking ability, photophysical properties, charge carrier mobility and photovoltaic performance, Macromolecules 43 (2010) 1261–1269.

[18] D.A.M. Egbe, G. Adam, A. Pivrikas, A.M. Ramil, E. Birckner, V. Cimrova, H. Hoppe, N.S. Sariciftci, Improvement in carrier mobility and photovoltaic performance through random distribution of segments of linear and branched side chains, Journal of Materials Chemistry 20 (2010) 9726–9734.

[19] S. Rathgeber, J. Perlich, F. Kühnlenz, S. Türk, D.A.M. Egbe, H. Hoppe, R. Gehrke, Correlation between polymer architecture, mesoscale structure and photovoltaic performance in side-chain-modified poly(p-arylene-ethynylene)-alt-poly(p-arylene-vinylene):PCBM bulk-heterojunction solar cells, Polymer 52 (2011) 3819–3826.

[20] S.E. Shahaen, C.J. Brabec, N.S. Sarıciftci, F. Padinger, T. Fromherz, J.C. Hummelen, 2.5% efficient organic plastic solar cells, Applied Physics Letters 78 (2001) 841–848.

[21] G. Li, V. Shrotriya, Y. Yao, Y. Yang, Investigation of annealing effects and film thickness dependence of polymer solar cells based on P3HT, Journal of Applied Physics 98 (2005) 043704–043709.

[22] R. Bettignies, S. Guillerez, Cathode composition greatly influences the life time of organic photovoltaic cells, International Society for Optical Engineering (2006), http://dx.doi.org/10.1117/2.1200606.0307. SPIE Newsroom.

[23] E.A. Parlak, The blend ratio effect on the photovoltaic performance and stability of poly(3-hexylthiophene):[6,6]-phenyl-C_{61} butyric acid methyl ester (PCBM) and poly(3-octylthiophene):PCBM solar cells, Solar Energy Materials and Solar Cells 100 (2012) 174–184.

[24] M.O. Reese, S.A. Gevorgyan, M. Jorgersen, E. Bundgaard, S.R. Kurtz, D.S. Ginley, D.C. Olson, M.T. Lıold, P. Morvillo, E.A. Katz, A. Elschner, O. Haillant, T.R. Currier, V. Shrotriya, M. Hermenau, M. Riede, K.R. Kirov, G. Trimmel, T. Rath, O. Inganas, F. Zhang, M. Andersson, K. Tvingstedt, M. Lira-Cantu, D. Laird, C. McGuiness, S.M. DeLongchamp, R. Rosch, H. Hoppe, N. Espinosa, A. Urbina, G.Y. Uzunoglu, J.-B. Bonekamp, A.J.J.M. van Breemen, C. Girotto, E. Voroshazi, F.C. Krebs, Consensus stability testing protocols for organic photovoltaic materials and devices, Solar Energy Materials and Solar Cells 95 (2011) 1253–1267.